RADC-TR-85-241
In-House Report
December 1985

PRINTED CIRCUIT TRANSMISSION LINE TRANSITIONS

Frank E. Kozak, C1C, USAF
Daniel T. McGrath, Capt, USAF

ROME AIR DEVELOPMENT CENTER
Air Force Systems Command
Griffiss Air Force Base, NY 13441-5700

This report has been reviewed by the RADC Public Affairs Office (PA) and is releasable to the National Technical Information Service (NTIS). At NTIS it will be releasable to the general public, including foreign nations.

RADC-TR-85-241 has been reviewed and is approved for publication.

APPROVED: Paul H. Carr

PAUL H. CARR, Acting Chief
Antennas & RF Components Branch
Electromagnetic Sciences Division

APPROVED: Allan C. Schell

ALLAN C. SCHELL
Chief, Electromagnetic Sciences Division

FOR THE COMMANDER: John A. Ritz

JOHN A. RITZ
Plans Office

If your address has changed or if you wish to be removed from the RADC mailing list, or if the addressee is no longer employed by your organization, please notify RADC (EEAA) Griffiss AFB NY 13441-5700. This will assist us in maintaining a current mailing list.

Do not return copies of this report unless contractual obligations or notices on a specific document requires that it be returned.

Unclassified

SECURITY CLASSIFICATION OF THIS PAGE

REPORT DOCUMENTATION PAGE

1a REPORT SECURITY CLASSIFICATION: Unclassified	1b RESTRICTIVE MARKINGS
2a SECURITY CLASSIFICATION AUTHORITY	3 DISTRIBUTION/AVAILABILITY OF REPORT: Approved for public release; Distribution unlimited.
2b DECLASSIFICATION/DOWNGRADING SCHEDULE	
4 PERFORMING ORGANIZATION REPORT NUMBER(S): RADC-TR-85-241	5. MONITORING ORGANIZATION REPORT NUMBER(S)
6a NAME OF PERFORMING ORGANIZATION: Rome Air Development Center; 6b OFFICE SYMBOL (If applicable): EEAA	7a NAME OF MONITORING ORGANIZATION
6c. ADDRESS (City, State and ZIP Code): Hanscom AFB, Massachusetts 01731	7b. ADDRESS (City, State and ZIP Code)
8a NAME OF FUNDING/SPONSORING ORGANIZATION: Rome Air Development Center; 8b. OFFICE SYMBOL (If applicable): EEAA	9. PROCUREMENT INSTRUMENT IDENTIFICATION NUMBER
8c ADDRESS (City, State and ZIP Code): Hanscom AFB, Massachusetts 01731	10 SOURCE OF FUNDING NOS.

PROGRAM ELEMENT NO.	PROJECT NO.	TASK NO.	WORK UNIT NO.
62702F	4600	14	02

11 TITLE (Include Security Classification.) Printed Circuit Transmission Line Transitions

12. PERSONAL AUTHOR(S): Frank E. Kozak, C1C, USAF and Daniel T. McGrath, Capt, USAF

13a TYPE OF REPORT	13b TIME COVERED	14 DATE OF REPORT (Yr., Mo., Day)	15. PAGE COUNT
In-house	FROM _____ TO _____	1985 December	30

16. SUPPLEMENTARY NOTATION

17 COSATI CODES			18 SUBJECT TERMS (Continue on reverse if necessary and identify by block number)
FIELD	GROUP	SUB GR	Microstrip antennas; Printed circuit antennas; Conformal antennas; Transmission lines
09	03		

19 ABSTRACT (Continue on reverse if necessary and identify by block number)

Three types of printed circuit transmission lines were investigated experimentally: microstrip; stripline; and grounded coplanar waveguide. Formulas for characteristic impedance were verified by measurements of lines on low-dielectric-constant substrates.

Several designs of transitions from coaxial cable to microstripline were tested. The best of these was a uniform microstripline with a flare at the connector end. A transition from coax into coplanar waveguide, and one from stripline into microstrip, had high reflection coefficients. Transitions from coax to stripline, and from coplanar waveguide to microstrip, had low reflection coefficients.

20 DISTRIBUTION/AVAILABILITY OF ABSTRACT	21 ABSTRACT SECURITY CLASSIFICATION
UNCLASSIFIED/UNLIMITED ☐ SAME AS RPT ☒ OTIC USERS ☐	Unclassified

22a NAME OF RESPONSIBLE INDIVIDUAL	22b TELEPHONE NUMBER (Include Area Code)	22c OFFICE SYMBOL
Daniel T. McGrath, Capt, USAF	(617) 861-4036	RADC/EEAA

DD FORM 1473, 83 APR EDITION OF 1 JAN 73 IS OBSOLETE

Unclassified

SECURITY CLASSIFICATION OF THIS PAGE

Preface

This report is a summary of work performed at Rome Air Development Center's Electromagnetic Sciences Division. Cadet Frank Kozak's participation was made possible by the United States Air Force Academy's (USAFA) Summer Research Program. Capt Daniel Martin was the liaison for the USAFA Department of Electrical Engineering. Capt Daniel McGrath (RADC/EEA) was the sponsor and co-investigator.

Contents

Illustrations

Printed Circuit Transmission Line Transitions

1. INTRODUCTION

Printed circuit transmission lines are quasi-TEM waveguiding structures used to carry radio frequency signals over short distances. The particular application of those structures that we are most interested in are power divider networks and array antennas. Their advantages over other types of transmission lines are best realized when the entire antenna is constructed as a printed circuit, similar to that shown in Figure 1. The savings in cost, ease of fabrication, weight, and small size outweigh the disadvantage of higher loss relative to coaxial cable or rectangular waveguide.

The purposes of this research project were: (1) verify published formulas for design of printed circuit transmission lines and (2) test several designs of transitions from coax to microstripline. In particular, we proposed three ways of improving the transition from coax to microstrip: (1) taper or miter the end of the microstripline to keep its corners away from the flange of the coaxial launcher (2) transition first into a short section of stripline, and then transition from stripline to microstrip; and (3) launch into a short section of coplanar waveguide with a constant-impedance transition to microstrip.

(Received for publication 6 December 1985)

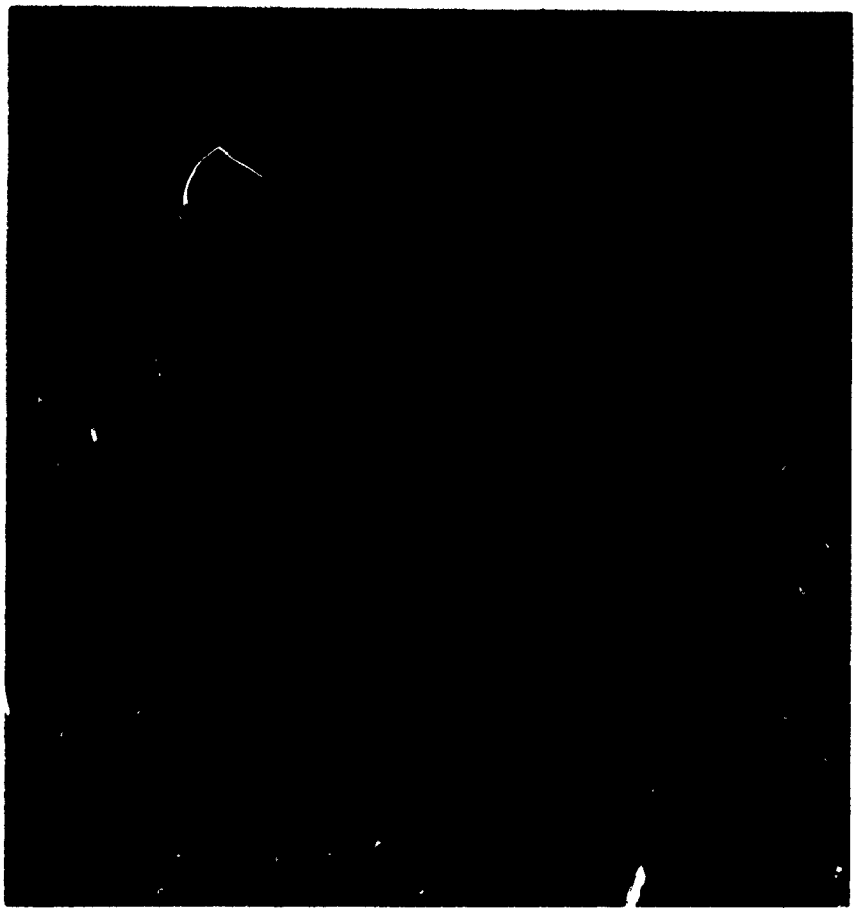

Figure 1. Printed Circuit Array Antenna
(Courtesy Ball Aerospace)

2. BACKGROUND

Two major sources of loss in microstrip antennas and circuits are (1) radiation and reflection from discontinuities and (2) dissipation in the conductors and in the dielectrics. There are formulas for calculating the dissipative losses, but there is little published information on the losses due to discontinuities, in particular the transitions from coaxial cable into microstrip. Such transitions are inevitable in our microstrip research because we can only test the properties of an antenna or microwave device using a network analyzer or a receiver, both of which have coaxial test ports. Two examples are shown in Figure 2. The rectangular microstrip patch antenna and the reactive power divider both have SMA coaxial connectors. In some of our earlier experiments with such devices, we could not accurately

measure the characteristics of the devices themselves, because of strong reflections from the coax-to-microstrip transitions at the board edges.

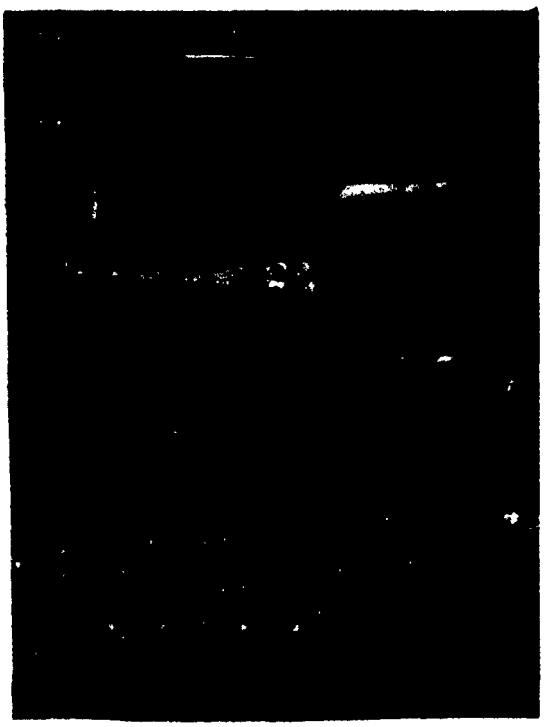

Figure 2. Microstrip Patch Antenna and Wilkinson Power Divider

The three types of printed circuit transmission lines of interest to this project are shown in Figure 3. Stripline is a flat conductor suspended between two ground planes by dielectric slabs. Microstrip is a similar conductor over a single ground plane. Coplanar waveguide is a single conductor inside a slot in the ground plane on top of the dielectric slab. The figure also shows the structure of the electric and magnetic fields of the transmission media.

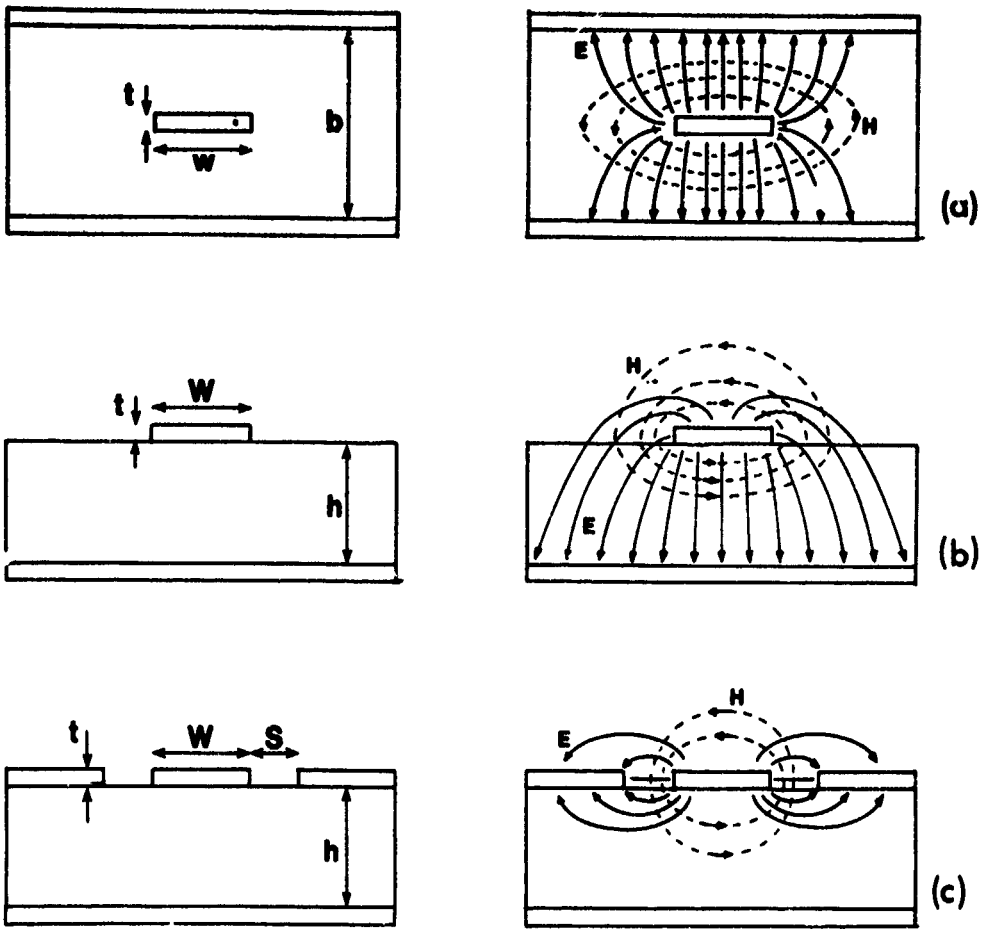

Figure 3. Transmission Line Geometry and Field Structure: (a) Stripline, (b) Microstrip, and (c) Coplanar Waveguide

3. DESIGN FORMULAS

3.1 Microstrip

The characteristic impedance of a microstripline of width W, on a substrate of thickness h and dielectric constant ϵ_r, and foil thickness t is [1:62]:

$$Z_o = \begin{cases} \dfrac{\eta}{2\pi\sqrt{\epsilon_{eo}}} \ln\left[\dfrac{8h}{W_e} + 0.025\,\dfrac{W_e}{h}\right] & \dfrac{W}{h} \leq 1 \\ \dfrac{\eta}{\sqrt{\epsilon_{eo}}}\left[\dfrac{W_e}{h} + 1.393 + 0.667\,\ln\left(\dfrac{W_e}{h} + 1.444\right)\right]^{-1} & \dfrac{W}{h} \geq 1 \end{cases} \quad (1)$$

where η is the impedance of free space, 376.7 Ω. W_e is the effective line width, which accounts for fringing of the fields near the strip edge, as well as for the foil thickness:

$$W_e = W + 1.25t\,\delta/\pi \quad (2a)$$

$$\delta = \begin{cases} 1 + \ln(4\pi W/t) & W/h \leq 0.5/\pi \\ 1 + \ln(2h/t) & W/h \geq 0.5/\pi \end{cases} . \quad (2b)$$

The effective dielectric constant for DC frequency is ϵ_{eo} (sometimes denoted ϵ_{re}):

$$\epsilon_{eo} = \frac{\epsilon_r + 1}{2} + \frac{\epsilon_r - 1}{2}\left[1 + 10\,\frac{h}{W}\right]^{-1/2} + \frac{\epsilon_r - 1}{4.6}\,\frac{t/h}{\sqrt{W/h}} . \quad (3)$$

Figure 4 shows how the characteristic impedance varies with the microstripline's width for two different dielectrics, Rexolite and epoxy-fiberglas, with relative dielectric constants, ϵ_r, of 2.54 and 4.4, respectively.

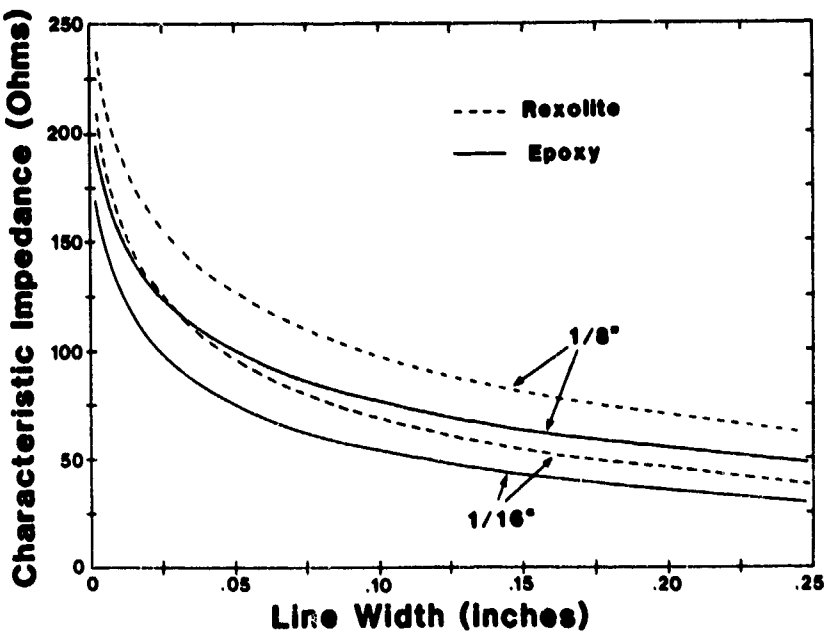

Figure 4. Characteristic Impedance of Microstrip

3.2 Stripline

The following formula gives the characteristic impedance of a stripline of width W and thickness t, suspended an equal distance b/2 between two ground planes [1:57]:

$$Z_o = \frac{30}{\sqrt{\epsilon_r}} \ln \left\{ 1+\beta \left[2\beta + \sqrt{4\beta^2 + 6.27} \right] \right\} \tag{4a}$$

$$\beta = \frac{4(b-t)}{\pi W_e} \tag{4b}$$

$$W_e = W + \frac{x(b-t)}{\pi(1-x)} \left\{ 1 - 0.5 \ln \left[\left(\frac{x}{2-x} \right)^2 + \left(\frac{0.0796\, x}{W/b + 1.1x} \right)^m \right] \right\} \tag{4c}$$

$$x = t/b \tag{4d}$$

$$m = 6(1-x)/(3-x)\,. \tag{4e}$$

W_e in Eq. (4c) is an effective line width that accounts for the fringing of fields in the vicinity of the line as illustrated in Figure 3a. Characteristic impedance vs stripline width is graphed in Figure 5 for Rexolite and epoxy.

3.3 Coplanar Waveguide

As originaliy proposed, coplanar waveguide (CPW) was two parallel slots on top of a semi-infinite dielectric slab.[1] Later, formulas were developed for the CPW on a substrate of finite thickness, h. In the following, K(k) and K'(k) represent the complete elliptic integrals of first and second kind. First, we calculate an effective dielectric constant, ϵ_{eff}:[2]

---

1. Wen, C. P. (1969) Coplanar waveguide: a surface strip transmissio.. line suitable for non-reciprocal gyromagnetic device application, IEEE Trans. Microwave Theory Tech., MTT-17:1087-1090.
2. Kitazawa, T. (1976) A coplanar waveguide with thick metal coating, IEEE Trans. Microwave Theory Tech., MTT-24:604-608.

$$\epsilon_{eff} = 1 + \frac{\epsilon_r - 1}{2} \frac{K'(k)}{K(k)} \frac{K(k_1)}{K'(k_1)} \tag{5a}$$

$$k_1 = \frac{\sin h(\pi W/4h)}{\sin h[\pi(W+2S)/4h]} \tag{5b}$$

$$k = W/(W+2S) .$$

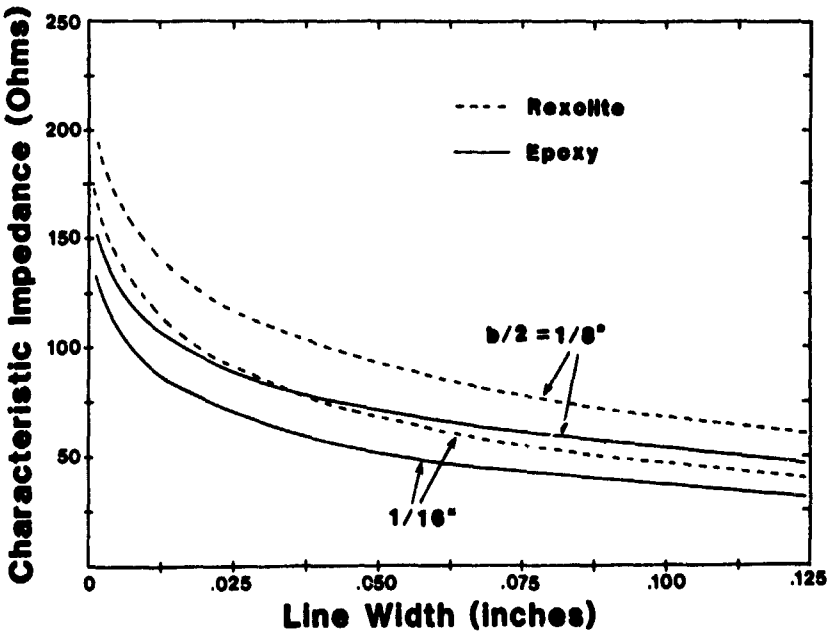

Figure 5. Characteris ic Impedance of Stripline

An ac curate approximation for the ratio of elliptic integrals is [1;57]:

$$K(k)/K'(k) = \begin{cases} \left\{ 1/\pi \ln[(2+2\sqrt{k'})/(1-\sqrt{k'})] \right\}^{-1} & 0 \leq k \leq 0.7071 \\ 1/\pi \ln[(2+2\sqrt{k})/(1-\sqrt{k})] & 0.7071 \leq k \leq 1 . \end{cases} \tag{5c}$$

$$k' = \sqrt{1 - k^2} .$$

To account for the thickness of the foil, we calculate a second effective dielectric constant, as well as compensated values for S, W and k:

$$\delta = 1.25t/\pi \left[1 + \ln(4\pi W/t)\right]$$

$$S_e = S + \delta \; ; \; W_e = W + \delta \; ; \; k_e = W_e/(W_e + 2S_e)$$

$$\epsilon_{eft} = \epsilon_{eff} - \frac{(\epsilon_{eff} - 1)}{\frac{S}{0.7t}\frac{K(k)}{K'(k)} + 1} \tag{5d}$$

$$Z_o = \frac{30\pi}{\sqrt{\epsilon_{eft}}} \frac{K'(k_e)}{K(k_e)} \; . \tag{5e}$$

Figure 6 shows the characteristic impedance of a coplanar waveguide vs the ratio of slot width to conductor width for several dielectric materials with h >>W+2S.

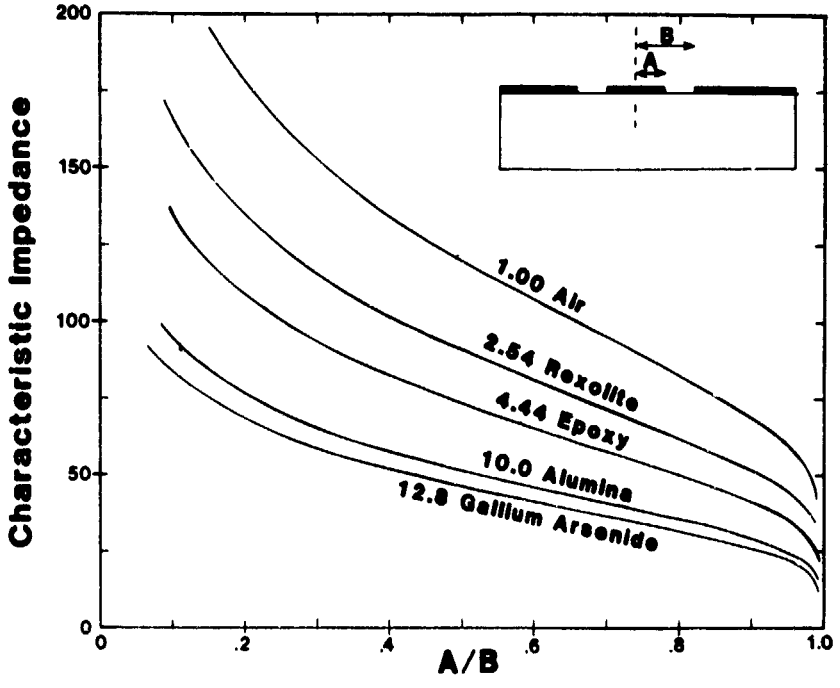

Figure 6. Characteristic Impedance of Coplanar Waveguide on a "Thick" Substrate (h >> W + 2S). A = W/2, B = S + W/2.

3.4 Grounded Coplanar Waveguide

The difficulty with CPW is that previous formulas only applied to semi-infinite dielectrics, or finite-thickness dielectrics suspended in free space. Only recently have Rowe and Lao[3] derived expressions for a coplanar waveguide on top of a grounded dielectric. Their expression gives the characteristic impedance in the general form of a microstripline impedance in parallel with a CPW impedance:

$$Z_o = \left[\frac{5q}{1+5q} \frac{1}{Z_m} + \frac{1}{1+q} \frac{1}{Z_c} \right]^{-1} \tag{6a}$$

$$q = W/h[(W+2S)/W - 1] \quad \{3.6 - 2 \exp[-(\epsilon_r + 1)/4]\} . \tag{6b}$$

Z_m and Z_c are, respectively, the microstrip and CPW impedances from Eqs. (1) and (5e). Figure 7 shows three contours of constant impedance for a CPW on grounded Rexolite dielectric 1/16-in. thick. Note that as the slot width grows large, the center conductor width approaches the width of a microstripline on the same substrate. Figure 8 shows a constant impedance transition from CPW to microstrip: at every point the combination of slot width and center conductor width yields 50Ω. This was one of our experimental transitions—the center conductor width at the narrow end is the same as that of 50Ω coax.

4. EXPERIMENTS

4.1 Procedures

The artwork for the circuits was drawn to 200 percent actual size on the Calcomp plotter with a liquid ink pen. The photographic negative used in photo-etching was shot to actual size. The artwork included the outline and hole pattern for the test fixture, to make sure the circuit was aligned properly.

Figure 9 shows a microstripline mounted in the aluminum test fixture. The SMA jack-tab connectors are mounted with screws on either end of the fixture, with the tab soldered to the transmission line. Nylon screws are used to hold the substrate flush with the aluminum fixture, which forms the ground plane.

All measurements were made using an HP8408 automatic network analyzer.

---

3. Rowe, D. A., and Lao, B. Y. (1983) Numerical analysis of shielded coplanar waveguide, IEEE Trans. Microwave Theory Tech., MTT-31:911-915.

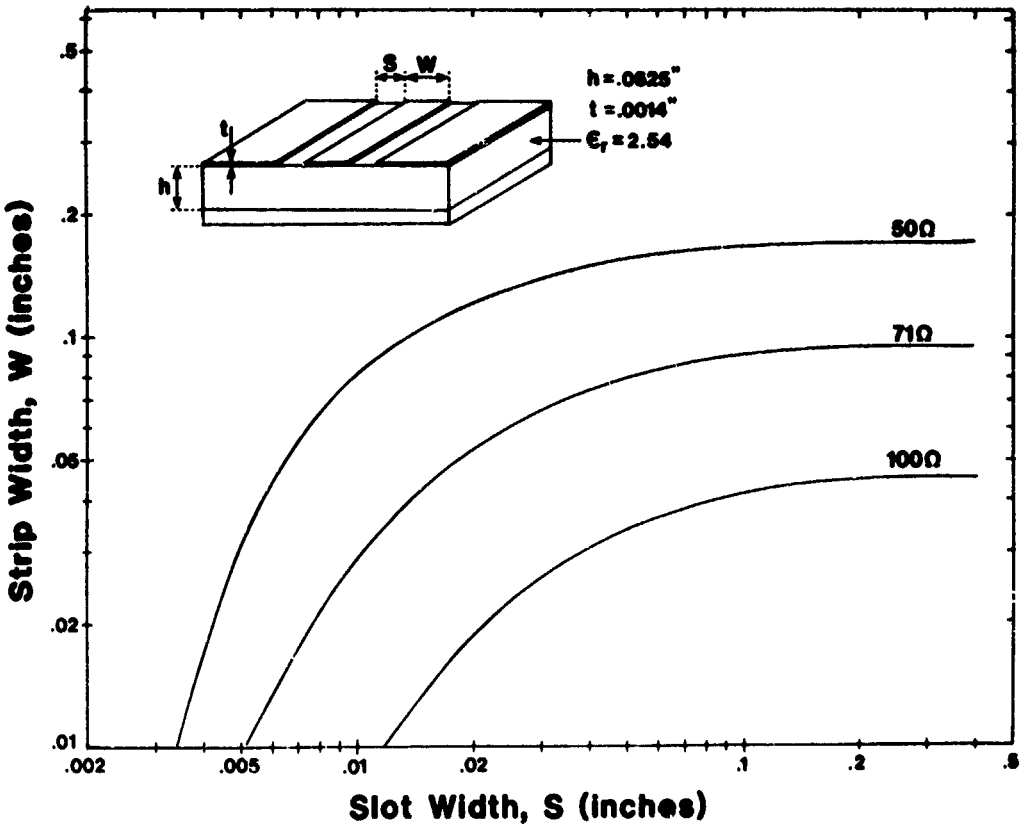

Figure 7. Characteristic Impedance of Grounded Coplanar Waveguide

4.2 Multiple Reflections and Reference Plane Extension

A typical measurement of return loss is shown in Figure 10a. The periodicity is the effect of two mismatches in series, illustrated schematically in Figure 10b. Figure 10c relates that to the actual circuit being measured: Z_1 and Z_2 are the discontinuities between the stripline and the coaxial connectors. The second connector is terminated with a 50Ω matched load, and we assume that it has zero reflection coefficient.

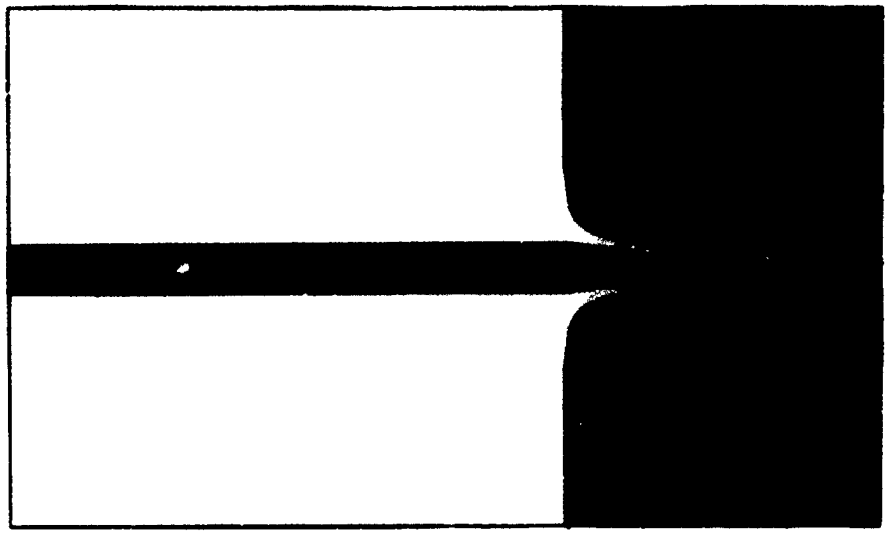

Figure 8. Constant-Impedance Transition From CPW to Microstrip

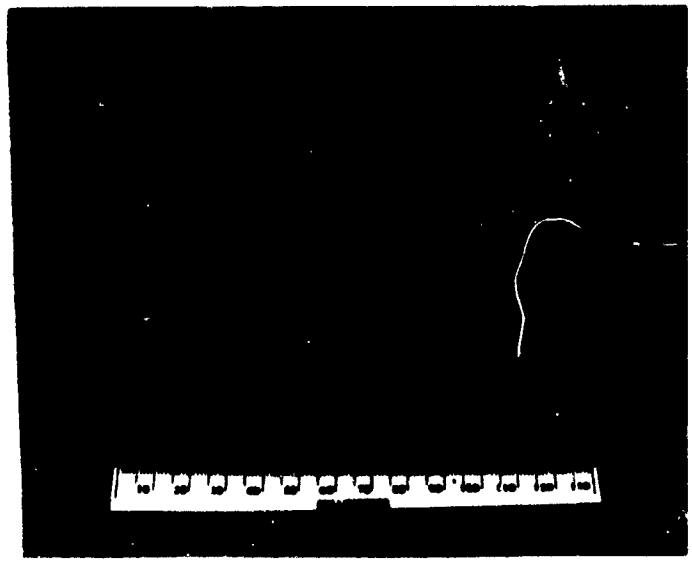

Figure 9. Test Fixture

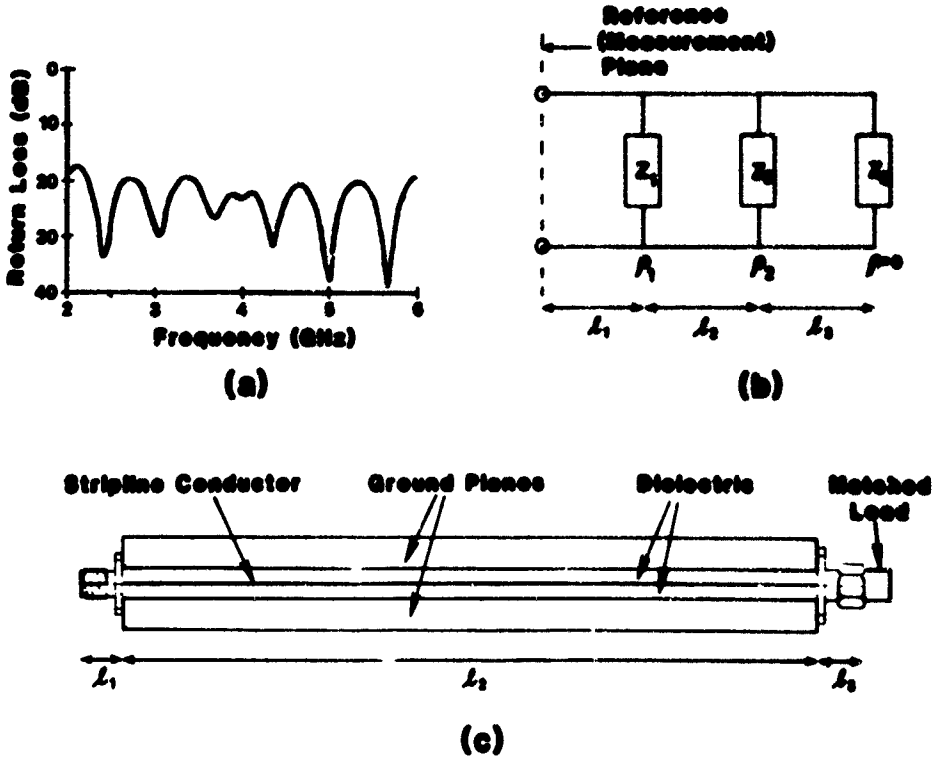

Figure 10. Reflection From Two Discontinuities: (a) Measured Return Loss, (b) Schematic Representation, and (c) Actual Circuit

The network analyzer injects a current I_i into the circuit and measures the returning current I_r. The reflection coefficient is $\rho_m = I_r/I_i$, which is a sum of all reflections in the circuit. We want to isolate ρ_1, the reflection coefficient of the first transition. Appendix A shows that the total reflection coefficient is:

$$\rho_m = e^{-j2\beta_1 l_1}\left[\rho_1 + \rho_2|1-\rho_2|^2\, e^{-2\alpha l_2}\, e^{-j2\beta_2 l_2}\right] \qquad (7)$$

(assuming the first section of coaxial line is lossless). The measured data from Figure 10a is plotted in polar form in Figure 11a. Figure 11b shows the same data with a phase correction of $+2\beta_1 l_1$. The result of that phase correction is that the measured data describes a circle about some central point on the polar plot, as shown in Figure 11b. That point is the vector ρ_1. The phase correction essentially moved the reference plane to the position of the first discontinuity.

This reference plane extension technique allows us to clearly identify ρ_1 in both magnitude and phase. Figure 11b is a measurement made on a stripline that was too narrow due to overreduction during photographing, and also a slight over-etching. The resulting line width of 0.073 in. corresponds to an impedance of 56.5 Ω. The center of the best fit circle in Figure 11b has a resistance component of $1.15 \times 50\,\Omega$, or 57.5 Ω.

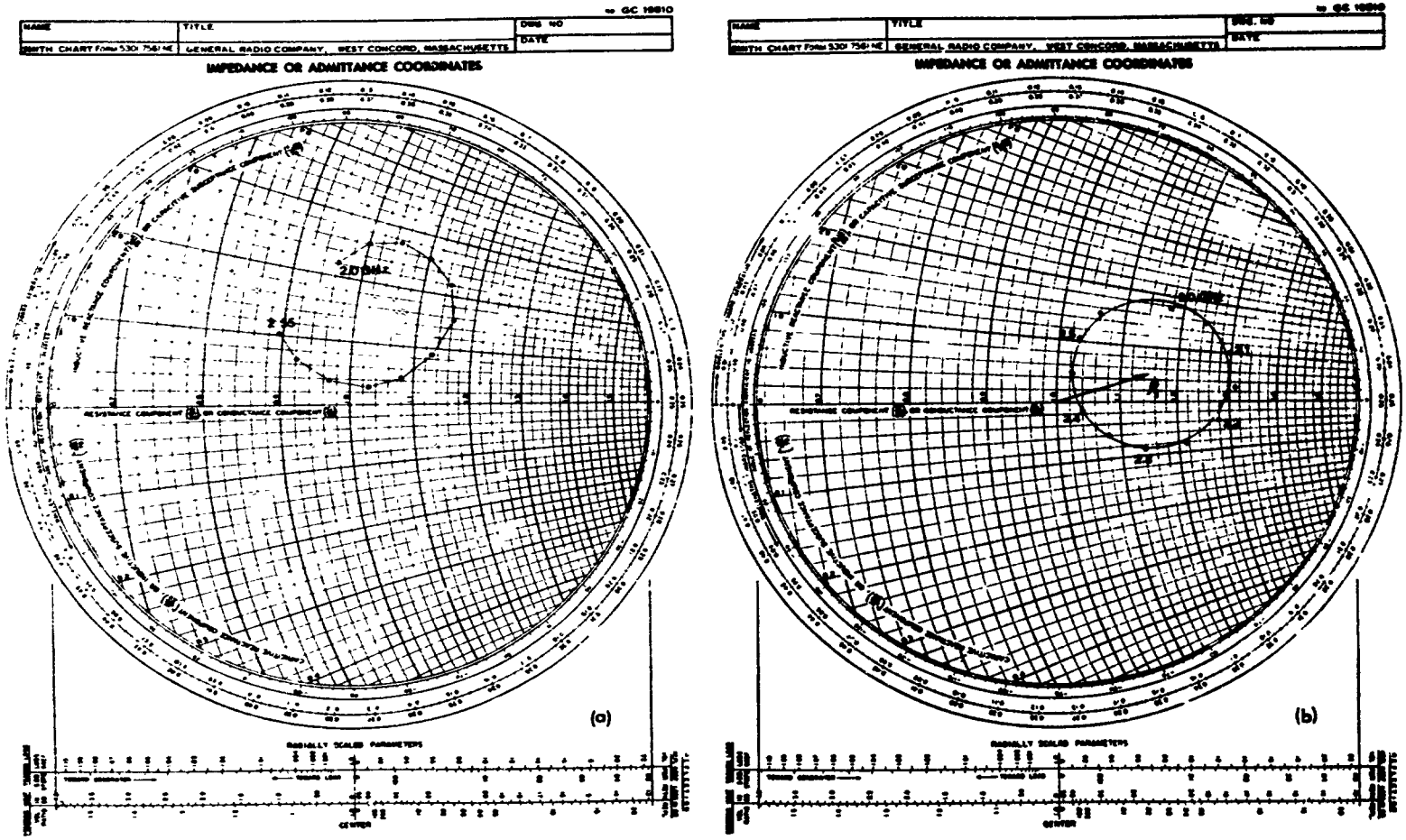

Figure 11. Impedance Plot of Stripline Reflection Coefficient: (a) Uncorrected and (b) With Reference Plane Extension

4.3 Measurements

4.3.1 MITERED MICROSTRIP

The mitered microstrip is a line of uniform width, except that near each connector, it is angled away from the connector's flange, as illustrated in Figure 12. We tested several versions, each with a different angle of miter, α. The measured reflection coefficients are shown in Figure 13. The 15°-mitered microstrip yields the lowest reflection coefficient over the frequency range from 8 to 18 GHz. Evidently, the slight miter of 15°, just enough to get the corners of the line away from the flange, reduces the stray inductance at the junction without changing Z_0. As the microstrip is mitered further, the characteristic impedance of the line near the connection grows larger, resulting in a mismatch between it and the 50Ω connector. We conclude that the best design of mitered microstrip transition is the 15° taper, although we do not know if this will hold true for other dielectrics and substrate thicknesses.

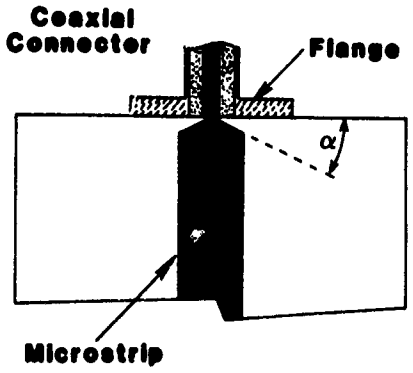

Figure 12. Mitered Microstrip Geometry

4.3.2 STRIPLINE TO MICROSTRIP

We expected to have no problem in matching a 50Ω stripline to the SMA connector because their dimensions are so similar. As Figure 14 shows, the reflection coefficient measured from the uniform stripline was slightly lower than the best microstrip case (15° miter).

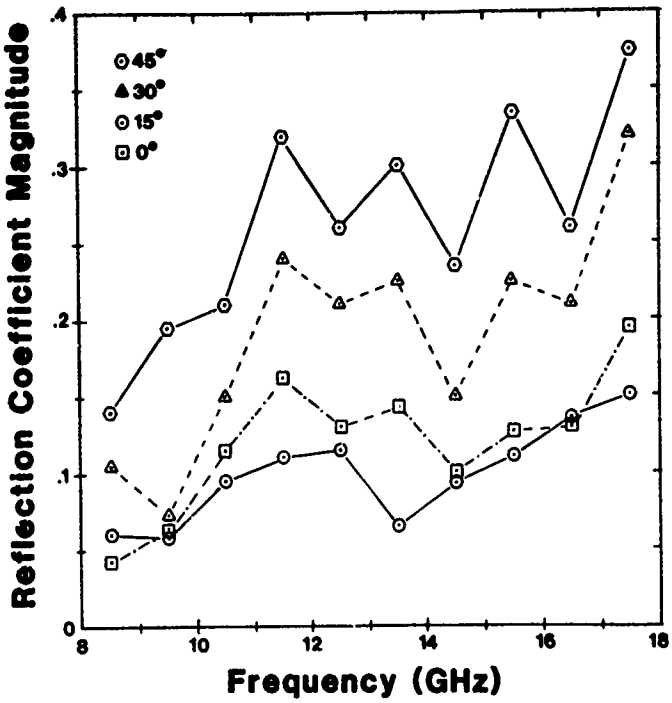

Figure 13. Measured Reflection Coefficient of Mitered Microstrip Lines

The stripline-to-microstrip transition is shown in Figure 15. At the edge of the fixture, the coax connector launches into a section of 50Ω stripline formed by a narrow conductor covered by a rectangular piece of copper-clad material. The right side of the circuit is shown with the cover piece removed. The transition is simply an abrupt truncation of the top ground plane of the stripline at the point where the conductor widens to the width of 50Ω microstripline. The results, shown in Figure 16 were rather disappointing. It is evident that the transition from the stripline to the microstrip introduces a very strong reflection. At some frequencies, it appears that the circuit is radiating from those discontinuities, or from the combination of the two discontinuities.

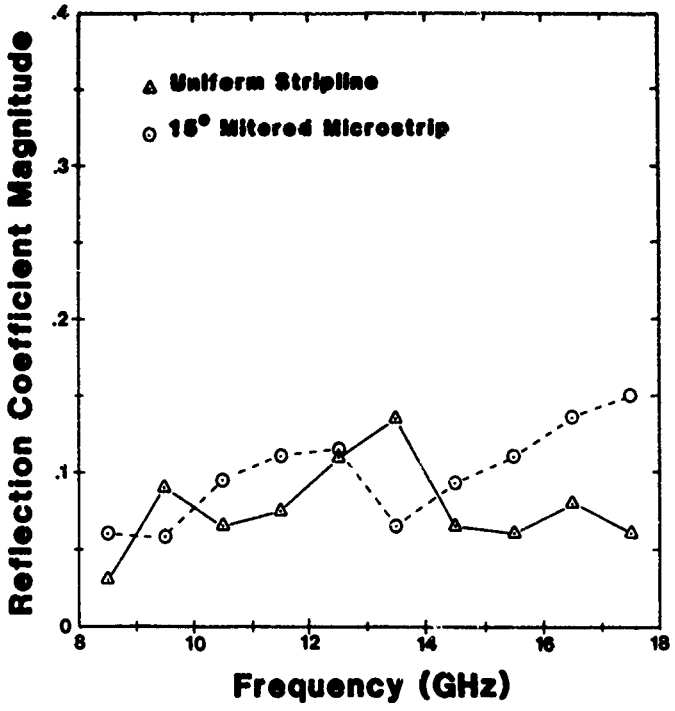

Figure 14. Stripline Reflection Coefficient

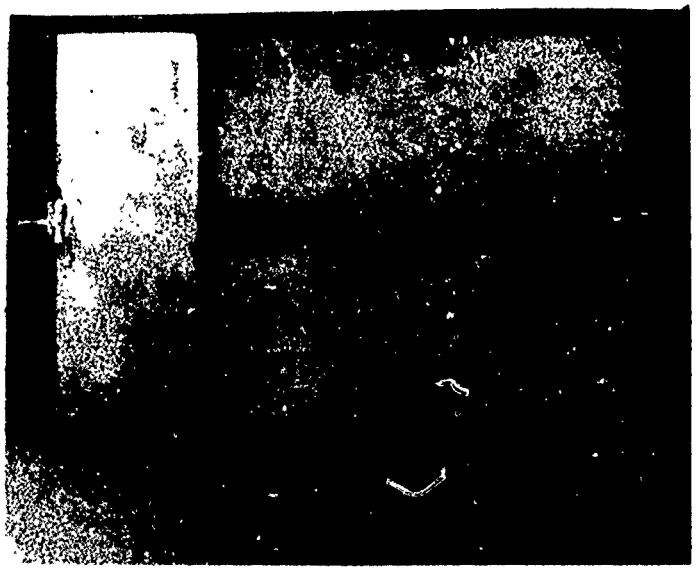

Figure 15. Stripline to Microstrip Transition

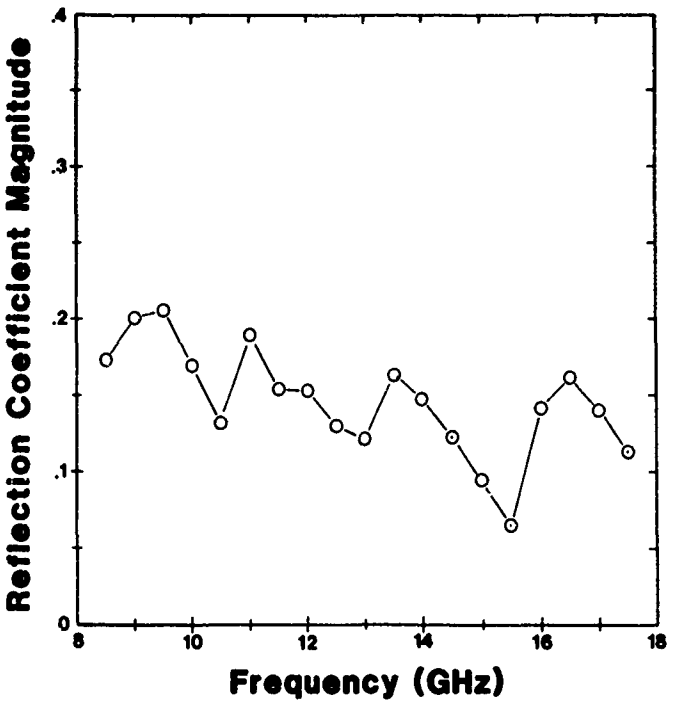

Figure 16. Measured Reflection Coefficient Stripline-Microstrip Transition

4.3.3 COPLANAR WAVEGUIDE TO MICROSTRIP

Figure 17 shows the measured reflection coefficient vs frequency for the CPW-microstrip transition of Figure 8, compared with the 15°-mitered microstrip. Although the CPW reflection coefficient is somewhat higher, the measured data show only the two mismatches at each end of the circuit. We conclude that the transition from CPW to microstrip can work properly, but there is a strong reflection from the CPW-coax junction.

4.4 Microstrip Dispersion

Microstripline is a dispersive transmission medium because the velocity of propagation along the line varies with frequency. The reason this is so is that the fringing fields are not enclosed in the substrate dielectric, but also penetrate the air above the substrate. Effectively, the dielectric constant will appear to be something in between that of air and that of the substrate's ϵ_r. As frequency changes, so does the structure of the fringing fields, resulting in a change in

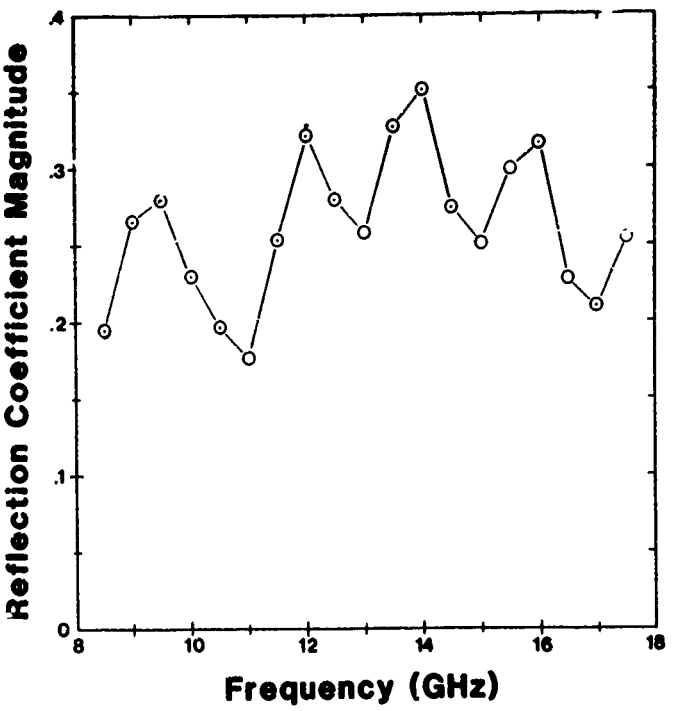

Figure 17. Measured Reflection Coefficient, Coplanar Waveguide - Microstrip Transition

effective dielectric constant. Gupta et al[4] give the following expression for the effective dielectric constant, from which we calculate the guide wavelength as $\lambda_g = \lambda_o / \sqrt{\epsilon_{eff}(f)}$ [1:63]:

$$\epsilon_{eff}(f) = \epsilon_r - (\epsilon_r - \epsilon_{eo})/[1+G(f/f_p)^2] \quad (8a)$$

where ϵ_{eo} is as given in Eq. (3) and:

$$G = \sqrt{(Z_o - 5)/60} + 0.004\, Z_o \quad (8b)$$

$$f_p(\text{GHz}) = 15.66\, Z_o / h(\text{mils}) \,. \quad (8c)$$

4. Gupta, K. C., Garg, R., and Chadha, R. (1981) Computer-Aided Design of Microwave Circuits, Artech House, Dedham, Massachusetts.

For our parameters of W = 0.17174 in., h = 0.0625 in. = 62.5 mils, t = 0.0014 in. (1 oz. copper clad), $\epsilon_r = 2.54$ and $Z_o = 50\Omega$, Eq. (8c) reduces to:

$$\epsilon_{eff}(f) = 2.54 - 0.417/[1 + 1.066(f/f_p)^2] \tag{9}$$

$$f_p = 12.528\ \text{GHz} .$$

Figure 18 shows the $\epsilon_{eff}(f)$ calculated from Eq. (8a) and the measured effective dielectric constant, which was reduced from measured insertion phase data as follows. The electrical length of the line is

$$l_e = \frac{c}{360}\frac{\Delta\phi}{\Delta f} \tag{10}$$

where c is the speed of light and $\Delta\phi$ is the change in insertion phase due to a change Δf in frequency. Knowing that the physical length of the line is $l_p = 6.000$ in., we calculate ϵ_{eff} from:

$$\epsilon_{eff} = (l_e/l_p)^2 \tag{11}$$

The measured and calculated ϵ_{eff} in Figure 18 disagree by about 10 percent. We believe the discrepancy is an inaccuracy in the formula for the effective dielectric constant for DC, given by Eq. (3), since the shape of the two curves match quite well, but seem to be offset.

5. CONCLUSIONS

Three types of printed circuit transmission lines have been investigated for possible use in constructing transitions to coax cable from microstrip. The best transition we found was the simplest: the microstrip with a tapered end, or 15° miter. The stripline-to-microstrip transition had much higher reflection than even the non-mitered microstrip, and hence does not offer any hope of a better transition. The CPW-microstrip transition seems to work properly, but the CPW itself is a poor match to the coaxial connector.

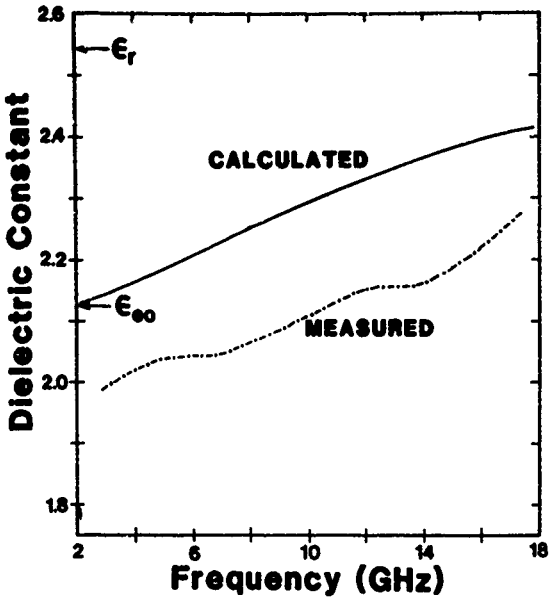

Figure 18. Calculated and Measured Effective Dielectric Constant for 50Ω Microstrip Line on Rexolite

In the course of these investigations, we have verified the design formulas for characteristic impedance of the microstrip, stripline and grounded coplanar waveguide. On the other hand, we have noted a disagreement with the published theory of effective dielectric constant of microstrip, and some further experimentation with other substrate materials will be needed to resolve the dispute.

Appendix A

Reflection From Two Discontinuities

When measuring the reflection coefficient of a circuit with two discontinuities, such as our printed circuit transmission lines, two phasors result. The situation is illustrated in Figure A1. The two discontinuities are the transitions from the coaxial test connectors to the transmission line. The second connector is terminated with a matched load, so we assume that there is no third reflection.

The measured reflection coefficient is $\rho_m = I_r/I_i$, where I_i is the current into the circuit and I_r is the total current reflected back out of the circuit, as observed by the network analyzer. Allowing for attenuation in the first length of line (coax) the current into the first connection is:

$$I_1 = I_i \exp[-j\beta_1 l_1] \exp[-\alpha_1 l_1] \tag{A1}$$

$$\beta = 2\pi\sqrt{\epsilon_r}/\lambda_o \ .$$

Of the current that reaches the first connection, I_{r1} is reflected back toward the source, which sees it phase shifted by twice the length of the first line section; and I_{t1} goes on to the second connection:

$$I_{r1} = I_i \exp[-j2\beta_1 l_1] \exp[-2\alpha_1 l_1] \tag{A2a}$$

$$I_{t1} = I_{i1}(1 - \rho_1) \ . \tag{A2b}$$

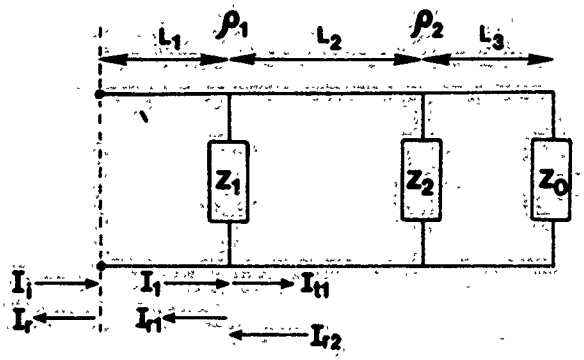

Figure A1. A Transmission Line Circuit With Two Discontinuities in Series

I_{r2} is the current returning to the first connector after traversing the test circuit and reflecting from the second connector:

$$I_{r2} = I_{t1} \exp[-j2\beta_2 l_2] \exp[-2\alpha_2 l_2] . \qquad (A3)$$

An amount $I_{r2}(1 - r_1)$ makes it through the first connector on its way back to the generator, with the result that the total reflection coefficient observed is:

$$\rho_m = e^{-2\alpha_1 l_1} e^{-j2\beta_1 l_1} [\rho_1 + \rho_2 |1 - \rho_1|^2 e^{-2\alpha_2 l_2} e^{-j2\beta_2 l_2}] . \qquad (A4)$$

The combination of these two phasors presents a problem in attempting to reduce the measured reflection data. As the polar plot of Figure A2a shows, as we change frequency, both vectors are rotating (since β is changing) and the resultant conveys little information. On the other hand, if we know l_1, then we can remove the effect of the first phasor simply by adding $2\beta_1 l_1$ to the measured phase. Neglecting the minor attenuation introduced by the first connector, Eq. (A4) reduces to:

$$\rho_m = [\rho_1 + \rho_2 |1 - \rho_1|^2 e^{-2\alpha_2 l_2} e^{-j2\beta_2 l_2}] . \qquad (A5)$$

Now, the measured data plotted in polar form is Figure A2b. The phase representing the second discontinuity is rotating about ρ_1, which is fixed. We can then accurately determine both the magnitude and phase of ρ_1 by fitting a circle to the measured data.

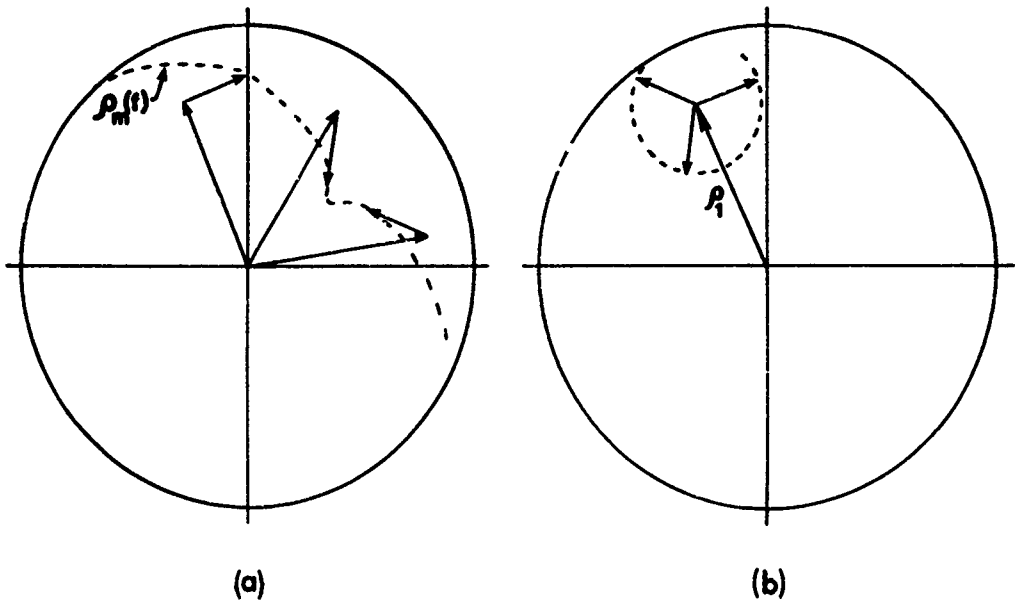

Figure A2. Polar Plot of Measured Reflection Coefficient vs Frequency: (a) Reference Plane at Measurement Plane and (b) Reference Plane at First Discontinuity

The physical length of the SMA coaxial connector (female, or "jack"), from the flange to the very top is 0.375 inch. The coax region is recessed 0.075 in. below the top. The dielectric material is Tetrafluoroethylene with a dielectric constant of about 2.1. Thus, its electrical length is approximately 0.435 inch.